ISSN 0915-633X

NATIONAL INSTITUTE FOR FUSION SCIENCE

Plasma Flow Measurement Using Directional Langmuir Probe under Weakly Ion-Magnetized Conditions

K. Nagaoka, A. Okamoto, S. Yoshimura and M.Y. Tanaka

(Received - June 22, 2000)

NIFS-638 July 2000

RESEARCH REPORT
NIFS Series

NAGOYA, JAPAN

Plasma Flow Measurement Using Directional Langmuir Probe Under Weakly Ion-Magnetized Conditions

Kenichi NAGAOKA, Atsushi OKAMOTO,
Shinji YOSHIMURA,[1] and Masayoshi Y. TANAKA[1]

Graduate School of Science, Nagoya University, Nagoya 464-8602, Japan
[1]*National Institute for Fusion Science, Toki 509-5292, Japan*

(Received June 21, 2000)

It is both experimentally and theoretically demonstrated that ion flow velocity at an arbitrary angle with respect to the magnetic field can be measured with a directional Langmuir probe. Based on the symmetry argument, we show that the effect of magnetic field on directional probe current is exactly canceled in determining the ion flow velocity, and obtain the generalized relation between flow velocity and directional probe currents valid for any flowing direction. The absolute value of the flow velocity is determined by an *in situ* calibration method of the probe. The applicability limit of the present method to a strongly ion-magnetized plasma is experimentally examined

KEYWORDS: plasma flow, directional Langmuir probe, Mach probe, magnetic field effect, calibration method, $E \times B$ drift

§1. Introduction

Measuring plasma flow velocity is of primary importance to study large-scale and self-organized structures in plasmas, and is also necessary to understand the dynamical behavior of surface plasma in confinement systems. So far, many works have been done on the flow velocity measurement using directional Langmuir probes (DLP) or Mach probes. Many of them are concerned with the parallel flow velocity measurements along the magnetic field,[1-3] and only a few works have been done on the perpendicular velocity measurement.[4-6] This is probably attributable to the fact that for the perpendicular velocity measurements, one have to anticipate the effect of magnetic field on the probe currents, which generally depends on the field intensity and/or direction in a complicated manner. Consequently, directional Langmuir probes have been considered to be unsuitable for the determination of perpendicular flow velocity.

Among many theoretical studies of DLP, Hudis and Lidsky extended the conventional probe theory to plasmas with a finite flow velocity and obtained that the Bohm criterion remains unchanged (free fall model).[7] Stangeby developed a fluid theory[1] for plasmas flowing along the magnetic field under strongly ion-magnetized conditions ($\rho_i/r_p \ll 1$), where ρ_i is ion Larmor radius, r_p probe radius. Hutchinson modified the fluid model,[2,8] and the results were confirmed by kinetic calculations.[3,9,10] Although these theories deal with parallel flow cases or unmagnetized cases, the results are merely adopted for the determination of perpendicular flow velocity without carefully examining the effect of magnetic field on the directional probe current.[11,12] Thus, the application of the conventional theory to perpendicular flow measurement has not been justified yet.

Moreover, DLP can not determine the absolute value of flow velocity, unless the calibration or crosscheck with a different method is made. For parallel flow case, Amagishi and Miyazaki showed that the difference of dispersion characteristic between a parallel propagating Alfven wave ($\boldsymbol{k} \parallel \boldsymbol{B}$) and an anti-parallel one ($\boldsymbol{k} \parallel -\boldsymbol{B}$) can be used for the calibration of a directional probe.[13] For perpendicular flow measurements, however, the situation is much more complicated than for the parallel case, and a different calibration method is required to determine the absolute flow velocity.

In this paper, we both experimentally and theoretically demonstrate that ion flow velocity at an arbitrary angle with respect to the magnetic field can be measured with a directional Langmuir probe. It is shown that the effect of plasma flow on the DLP current has odd property under the change of sign of flow velocity, while the effect of magnetic field has even property under the change of sign of magnetic field. Using the difference of symmetry property between flow and magnetic field effects, we can exactly cancel the effect of magnetic field, and derive the generalized formula between flow velocity and probe currents, valid for all flow directions. The experiments have been carried out to measure the perpendicular ion flow velocity, and the absolute value is determined by an *in situ* calibration method, in which the $E \times B$ drift velocities measured with a DLP are compared with that determined from the potential measurements with an emissive probe to specify the calibration constant. The experiments have also been done in a strongly ion-magnetized condition to examine the application limit of the present method. It is found that the limit is given by $\rho_i/r_p \sim 1$, which is understood as the onset of flow disturbance induced by the probe.

§2. Generalized relation between flow velocity and DLP currents

We consider a DLP in a magnetized plasma with the ion collecting surface whose normal of surface $\boldsymbol{n}$ is directed to a certain angle θ with respect to the reference frame (see Fig. 2(b) in §3). When there present no ion flow and no magnetic field, the ion saturation current, which is denoted here by $I_{\rm s}^{(0)}$, is given by the well-known formula. For a plasma with a finite ion flow velocity $\boldsymbol{V}$ and a magnetic field $\boldsymbol{B}$, the ion saturation current of DLP is modified from $I_{\rm s}^{(0)}$. However, when the changes in ion current are small enough compared with $I_{\rm s}^{(0)}$, the ion saturation current of DLP may be written as

$$I_{\rm s}(\boldsymbol{n}) = I_{\rm s}^{(0)}\big(1+F_V(\boldsymbol{V},\boldsymbol{n})\big)\big(1+F_B(\boldsymbol{B},\boldsymbol{n})\big), \qquad (2.1)$$

where F_V and F_B are the correction term due to the effects of ion flow and magnetic field, respectively. In the above equation, we make the hypothesis that the each effect is independent, and therefore the each contribution can be factorized as in eq.(2.1). This hypothesis is justified by the experimental result, which is given in §4.

The ion current of DLP should have the maximum for the case $\boldsymbol{n} \parallel -\boldsymbol{V}$ (the ion collection surface is faced to the upstream region) and have the minimum for the case $\boldsymbol{n} \parallel \boldsymbol{V}$ (the ion collection surface is faced to the downstream region). In other words, the function $F_V(\boldsymbol{V},\boldsymbol{n})$ has odd property under the change of sign of flow velocity $\boldsymbol{V}$ (or equivalently the change of sign of the normal vector $\boldsymbol{n}$). Then the scalar function F_V should be expanded in series of only odd powers of $\boldsymbol{V}\cdot\boldsymbol{n}$,

$$F_V = -\alpha_1(\boldsymbol{V}\cdot\boldsymbol{n}) - \alpha_3(\boldsymbol{V}\cdot\boldsymbol{n})^3 - \cdots, \qquad (2.2)$$

where α_n $(n = 1,3,\cdots)$ are positive expansion coefficients.

While the magnetic field effect does not distinguish the parallel $(\boldsymbol{B} \parallel \boldsymbol{n})$ and the anti-parallel $(\boldsymbol{B} \parallel -\boldsymbol{n})$ cases . The ion current of DLP is the same for the parallel and the anti-parallel cases, and should be minimum for the perpendicular cases $(\boldsymbol{B} \perp \boldsymbol{n})$, because the ion mobility is minimum in the perpendicular direction. This means that the scalar function F_B has even property under the change of sign of magnetic field $\boldsymbol{B}$ (or equivalently the change of sign of the normal $\boldsymbol{n}$). Then the function F_B should be expanded in series of only even powers of $(\boldsymbol{B}\cdot\boldsymbol{n})$,

$$F_B = \beta_2(\boldsymbol{B}\cdot\boldsymbol{n})^2 - \beta_4(\boldsymbol{B}\cdot\boldsymbol{n})^4 + \cdots, \qquad (2.3)$$

where β_n $(n = 2,4,\cdots)$ are expansion coefficients.

Collecting the leading order terms and rewriting eq.(2.1) in non-dimensional form, we have

$$I_{\rm s}(\boldsymbol{n}) = I_{\rm s}^{(0)}\Big(1-\alpha_1'\frac{\boldsymbol{V}}{C_{\rm s}}\cdot\boldsymbol{n}\Big)\Big(1+\beta_2'\frac{\rho_{\rm i}^2}{r_{\rm p}^2}(\boldsymbol{b}\cdot\boldsymbol{n})^2\Big), \qquad (2.4)$$

where $C_{\rm s}$ (ion sound velocity), $\rho_{\rm i}$ (ion Larmor radius), and $r_{\rm p}$ (DLP radius) are introduced to normalize the correction factors in non-dimensional forms. The vector $\boldsymbol{b}$ is the unit vector along the magnetic field. With the help of the even property of F_B $(F_B(\boldsymbol{n}) = F_B(-\boldsymbol{n}))$, we can eliminate the effect of magnetic field by making the quantity $I(\boldsymbol{n})/I(-\boldsymbol{n})$:

$$\frac{I_{\rm s}(\boldsymbol{n})}{I_{\rm s}(-\boldsymbol{n})} = \frac{I_{\rm s}(\theta)}{I_{\rm s}(\theta+\pi)} = \frac{1-\alpha_1'\dfrac{\boldsymbol{V}}{C_{\rm s}}\cdot\boldsymbol{n}}{1+\alpha_1'\dfrac{\boldsymbol{V}}{C_{\rm s}}\cdot\boldsymbol{n}}, \qquad (2.5)$$

where θ is the angle of normal of ion collection surface with respect to the reference frame.

The flow velocity is then obtained by solving this equation,

$$\frac{\boldsymbol{V}\cdot\boldsymbol{n}}{C_{\rm s}} = \frac{V\cos(\theta-\theta_{\rm d})}{C_{\rm s}} = \frac{1}{\alpha}\cdot\frac{I_{\rm s}(\theta+\pi)-I_{\rm s}(\theta)}{I_{\rm s}(\theta+\pi)+I_{\rm s}(\theta)}, \qquad (2.6)$$

where $\theta_{\rm d}$ is the angle of the flow velocity with respect to the reference frame, and the prime and subscript on α are omitted here.

It should be noted that eq.(2.6) is identical to the Stangeby's result with $\alpha = 0.5$ and $\theta = 0$ (parallel flow case). It is worth adding that our result is derived from the symmetry argument only, and is independent of the models under consideration (fluid model or free fall model). Equation (2.6) gives the generalized relation between the flow velocity and the DLP currents, and is valid for an arbitrary angle with respect to the magnetic field. Since the coefficient α may depend on the geometrical structure of DLP such as an aspect ratio of ion collection surface (see Fig. 2), the coefficient α has to be determined by calibration.

§3. Experimental Apparatus

The experiments have been performed in the High Density Plasma Experiment Device I (Hyper-I) at the National Institute for Fusion Science (NIFS), and the schematic of the Hyper-I device is shown in Fig. 1. The Hyper-I device consists of a cylindrical vacuum chamber (30cm in diameter and 200cm in axial length) and 10 magnetic coils to produce magnetic fields of 1kG along the chamber axis. A microwave of frequency 2.45GHz generated by a magnetron oscillator is converted to a circular $\rm TE_{11}$ mode and is introduced from an open end of the chamber through a tapered waveguide and a quartz window. The field coils are arranged to produce a weakly divergent magnetic field configuration, and the microwave launched from the strong field side excites an electron cyclotron wave, which produces and sustains the plasma by electron cyclotron resonance (ECR) heating. The ECR point (875G) locates near the central region of the chamber. At another end of the chamber, a three-dimensional (3D) probe drive system is installed to introduce an axial DLP. A radially movable DLP is introduced from the side port.

The microwave input power and plasma duration time are $4 \sim 15$kW and 1min., respectively. Three gas species, argon, helium and hydrogen, are used in the experiments, and the maximum density is $1\times10^{13}\rm cm^{-3}$ for argon. The electron and ion temperatures are $5 \sim 30$eV and ~ 1eV, respectively, with the operation pressure $0.1 \sim 2$mTorr.

The schematics of the directional Langmuir probe used in this experiment and the coordinate system are shown in Fig. 2. The DLP consists of a tungsten electrode and an alumina ($\rm Al_2O_3$) insulating tube of 3mm in diameter. The insulator has a small hole (1mm in diameter) on the

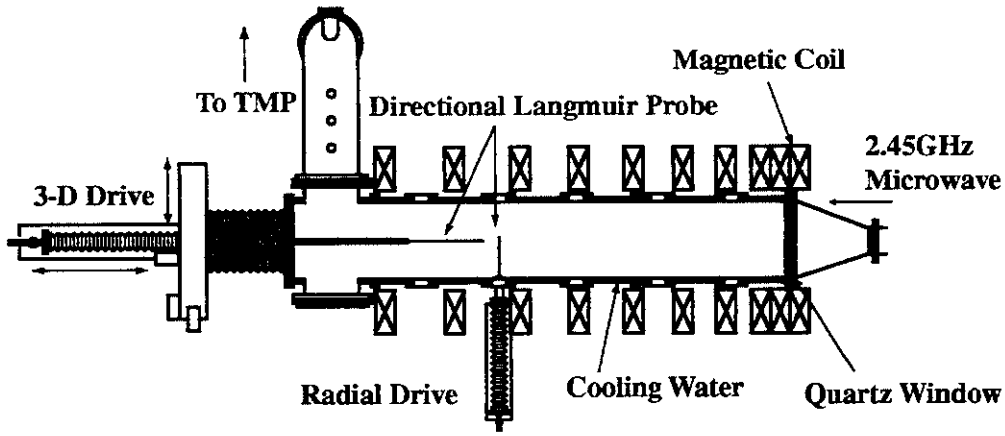

Fig. 1. Schematic of Hyper-I device.

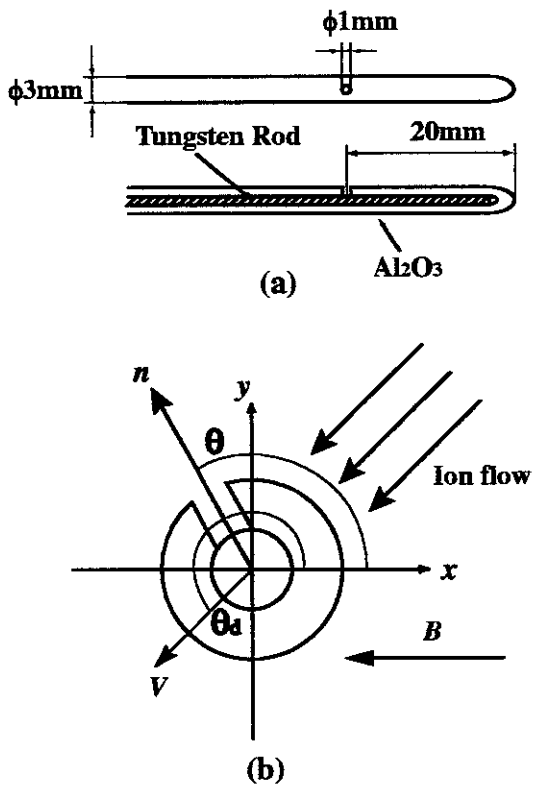

Fig. 2. (a): Schematic of directional Langmuir probe (DLP); (b): cut view of DLP and coordinate system. The x-axis is in the opposite direction to the magnetic field, and θ is the angle of normal of probe surface, and θ_d the angle of ion flow velocity with respect to the x-axis, respectively.

side surface to collect the directed ion flux. The reference frame, in which the x-axis coincides with the opposite direction of the magnetic field vector, is introduced, which is shown in Fig. 2(b). The angle of the normal of collector surface ($\boldsymbol{n}$) with respect to the x-axis is denoted by θ, and the angle of ion flow velocity by θ_d.

§4. Experimental Results

4.1 Effect of magnetic field on ion current of DLP

The ion saturation current of DLP as a function of probe angle θ is shown in Fig. 3, in which Fig. 3(a)~(c) are obtained for an argon plasma, and Fig. 3(d)~(f) for a helium plasma. In this figure, θ is the angle of the normal of collector surface with respect to the x-axis; $\theta = 0$ corresponds to the antiparallel case ($-\boldsymbol{B} \parallel \boldsymbol{n}$), $\theta = \pi$ the parallel case ($\boldsymbol{B} \parallel \boldsymbol{n}$), and $\theta = \pi/2$ and $3\pi/2$ the perpendicular case ($\boldsymbol{B} \perp \boldsymbol{n}$), with respect to the magnetic field. The ratio of ion Larmor radius to the probe radius is $(\rho_i/r_p) \sim 4$ for the argon plasma, and ~ 1.3 for the helium plasma. Thus the ions are considered to be unmagnetized for the argon case, and weakly magnetized for the helium case.

As seen in Fig. 3(a), there is a minimum at $\theta_{min} \sim 2.4$ radian and maximum at $\theta_{max} \sim \theta_{min} + \pi$. This result is understood as the effect of ion flow; when the DLP surface is parallel to the ion flow ($\boldsymbol{n} \parallel \boldsymbol{V}$), the ion current decreases, and when the DLP surface is anti-parallel to the ion flow ($-\boldsymbol{n} \parallel \boldsymbol{V}$) the ion current increases because the DLP surface faces to the ion flow. Since the quantity $I(\theta)$ is a periodic function with period 2π, we can resolve it into the Fourier components $e^{im\theta}$ ($m = 0, 1, 2, \cdots$), which are shown in Fig. 3(b). The average value of $I(\theta)$ ($m = 0$) is not shown in the figure. As is mentioned above, the $m = 1$ component is attributable to the ion flow effect.

The magnetic field effect on the DLP appears in $m = 2$ amplitude; since the ion mobility takes the maxima in the parallel cases ($\theta = 0, \pi$) and the minima in the perpendicular cases ($\theta = \pi/2, 3\pi/2$), the ion current $I(\theta)$ of DLP exhibits peaks and bottoms with every $\pi/2$ interval, which corresponds to $m = 2$ Fourier mode.

The presence of $m = 2$ component is more remarkable for the helium case. It is clearly seen in Fig. 3(d) that two peaks appear at $\theta = 0$ and π (parallel case), and two bottoms at $\theta = \pi/2$ and $3\pi/2$ (perpendicular case). Correspondingly, the $m = 2$ amplitude becomes as high as the $m = 1$ amplitude. However, with the help of the π periodicity of $m = 2$ mode, we can eliminate the magnetic field effect by taking the ratio $(I(\theta+\pi) - I(\theta))/(I(\theta+\pi) + I(\theta))$, and extract the flow effect only, which is shown in Fig. 3(c) and (f). As is predicted in §2, the quantity $(I(\theta+\pi)-I(\theta))/(I(\theta+\pi)+I(\theta))$ is completely fitted by a trigonometric function with a

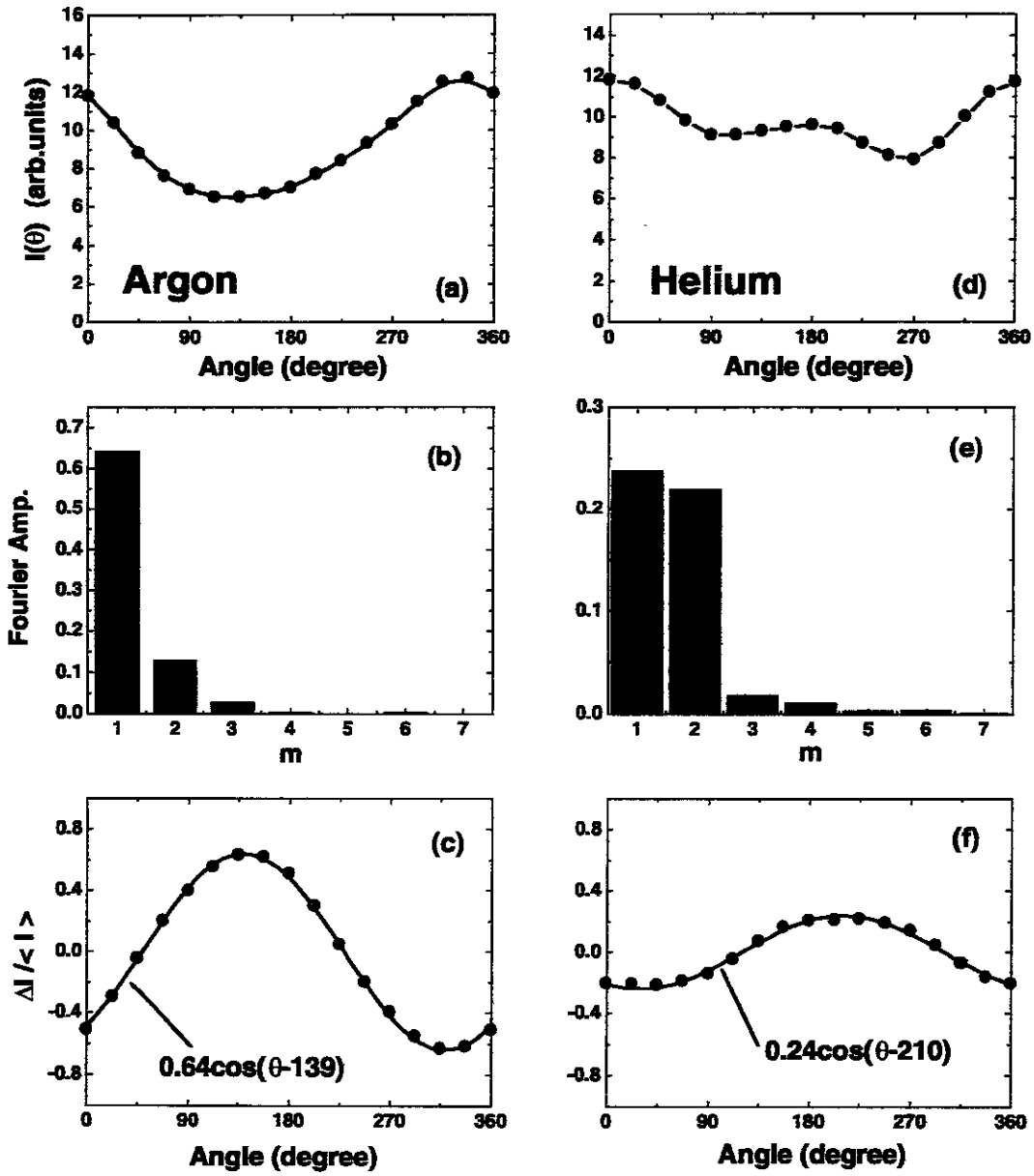

Fig. 3. Ion saturation current of DLP as a function of probe angle for an argon plasma (a)~(c), and for a helium plasma (d)~(f). Top: ion saturation current $I(\theta)$; middle: Fourier amplitude of $I(\theta)$; bottom: $\delta I/ < I >= 2(I(\theta+\pi) - I(\theta))/(I(\theta+\pi) + I(\theta))$. The best fit trigonometric functions are indicated in the bottom figures. Note that the amplitudes in (c) and (f) are proportional to the Mach number, and the phase shifts indicate the flow direction (see eq.(2.6)).

constant phase indicating the angle of flow direction. We emphasize that the $m = 2$ amplitude is the same order of magnitude as the $m = 1$ amplitude in the helium case. Thus we can conclude that the magnetic field effect can be removed even if it does exist in the same order of magnitude as the flow effect.

4.2 Absolute flow velocity

To determine the absolute value of ion flow velocity, we here present a simple calibration method of DLP. From the practical interest, it is preferable to specify the coefficient α in eq.(2.6) by an *in situ* calibration method. In this calibration procedure, the $E \times B$ drift velocity measured with a DLP is compared with that determined from the potential measurement using an emissive probe. The coefficient α is determined such that the value of DLP result equalizes to that obtained by the potential measurement.

Figure 4(a) shows the radial profile of ion currents measured at angles $\theta = \pi/2$ and $3\pi/2$, and the potential profile is given in Fig. 4(b). As seen in Fig. 4(a), the plasma rotates around the central axis ($x = 0$). The rotation velocity at each radial position is obtained by eq.(2.6). The $E \times B$ drift velocity is determined by numerically differentiating the potential profile and using the formula

$$\boldsymbol{V}_{E\times B} = \frac{-\nabla\phi \times \boldsymbol{B}}{B^2}, \tag{4.1}$$

which is indicated by closed circles in Fig. 5. The solid line indicates the velocity obtained by eq.(2.6) with the coefficient $\alpha = 0.45$. There is a quite good agreement between the two results, showing that the calibration of

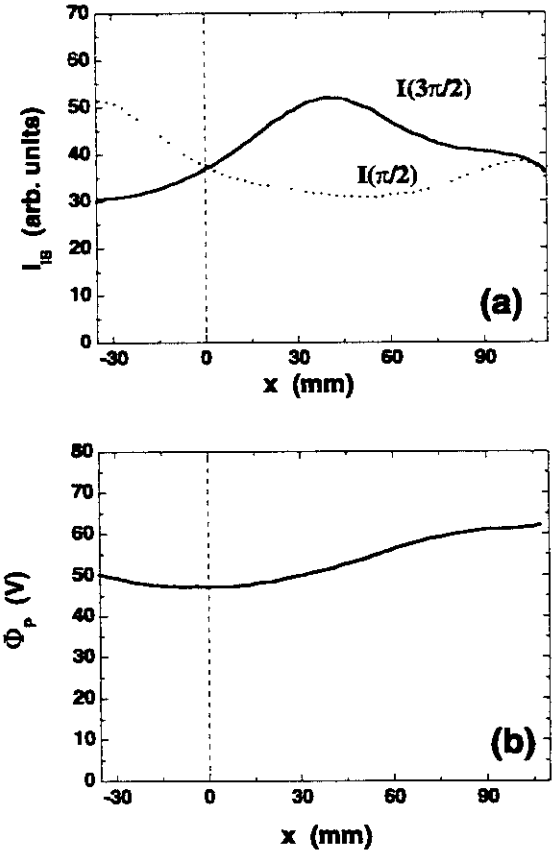

Fig. 4. (a): Radial profiles of DLP currents; (b): floating potential profile measured with an emissive probe .

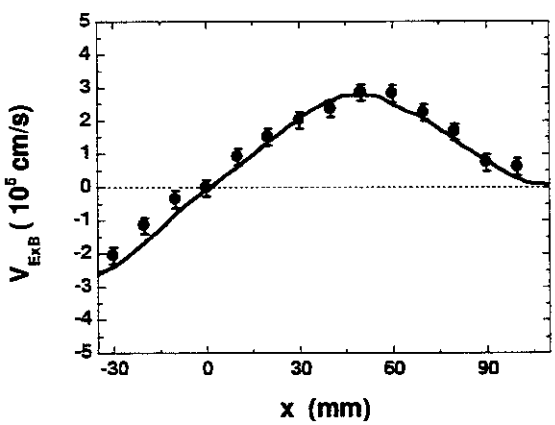

Fig. 5. Radial profile of $E \times B$ drift velocity. The closed circles indicate the results obtain from the potential measurement, and the solid line from eq.(2.6) with a coefficient $\alpha = 0.45$.

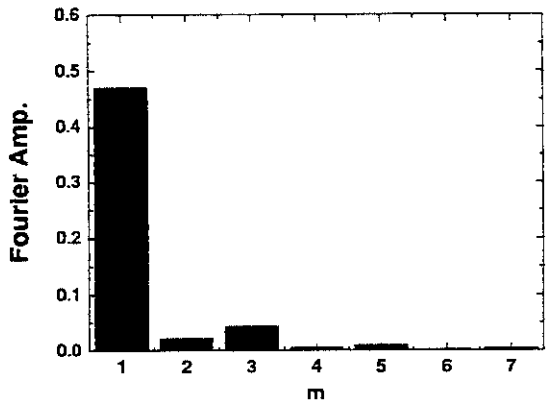

Fig. 6. Fourier amplitude of the quantity $I(\theta + \pi)/I(\theta)$.

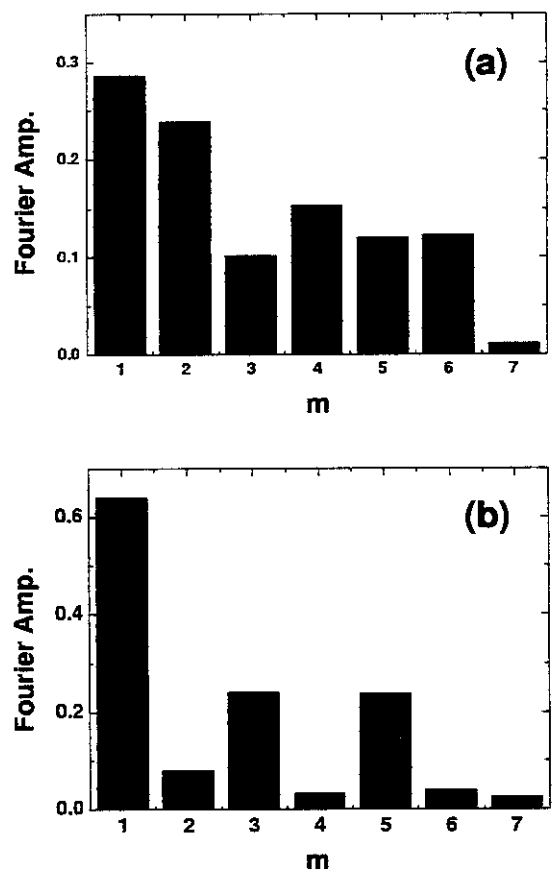

Fig. 7. (a): Fourier amplitude of DLP current $I(\theta)$ for a hydrogen plasma; (b): Fourier amplitude of the quantity $I(\theta + \pi)/I(\theta)$. The ratio of ion Larmor radius to DLP radius is $\rho_i/r_p \sim 0.7$.

DLP is successfully done. It is worth pointing out that the coefficient α is independent on radial positions although the electron temperature changes radially from 4eV to 25eV in this case. This suggests that the coefficient α is mainly determined by the geometrical factor.

§5. Discussion

We have demonstrated that the effect of magnetic field on DLP can be exactly eliminated, and the ion flow velocity at an arbitrary angle θ with respect to the magnetic field can be determined. The essential point which ensure the elimination of magnetic field effect is the factorized form of eq.(2.1), which we assumed without verification so far. Here we show the experimental verification for this hypothesis.

When those two effects are independent and therefore factorized, the ratio $I(\theta + \pi)/I(\theta)$ cancels the magnetic field effect because of even property of F_B. Then this quantity should have no even mode of Fourier amplitude $(m = 2, 4, 6, \cdots)$. Figure 6 shows the Fourier amplitude of the quantity $I(\theta + \pi)/I(\theta)$ made by the data given in Fig. 3(d). It is clearly seen in the figure that the even mode amplitudes $(m = 2, 4, 6, \cdots)$ are so small compared with Fig. 3(e), showing our hypothesis is actually valid.

To examine the applicability limit of our method to strongly ion-magnetized cases, we carried out the experiments using a hydrogen plasma ($\rho_i/r_p < 1$). Figure 7(a) shows the Fourier amplitude of the ion saturation current $I(\theta)$. As is expected, there present many higher Fourier amplitudes ($m = 3, 4, 5, \cdots$), however, the even modes ($m = 2, 4, 6, \cdots$) are canceled out in the quantity $I(\theta + \pi)/I(\theta)$. This suggests that the magnetic field effect still remain factorized and can be removed even in strongly ion-magnetized cases.

The appearance of higher Fourier components ($m = 3, 4, 5, \cdots$) is attributable to the disturbed flow induced by the DLP; since the ion Larmor radius ρ_i is smaller than the DLP radius r_p, the ion coming to the probe from the upstream region can not go into the downstream region, forming a shadow behind the probe, which generates a local electric field around the DLP and therefore modifies the original flow pattern by the disturbed $E \times B$ drift. It should be pointed out that the amplitude of $m = 1$ component is proportional to the flow velocity and can be extracted by Fourier analysis of $I(\theta)$ even in strongly ion-magnetized cases. However, the velocity measured in these circumstances may be a disturbed flow velocity, and much differ from the original one. From the practical viewpoint, the limit of applicability of DLP is considered to be $\rho_i \sim r_p$.

According to the discussion presented above, it is easily to know whether or not the flow velocity measurement with a DLP is possible. The validity of DLP method is justified by the condition that the DLP does not disturb the original flow, in other words, the higher Fourier components ($m \geq 3$) in DLP current is negligibly small. Therefore, we conclude that the DLP is valid as far as the higher mode Fourier amplitudes ($m \geq 3$) are negligible in the experiment.

The free fall model[7] and the fluid model[2] give a logarithmic form for the parallel flow velocity:

$$\frac{V_\parallel}{C_s} = \frac{1}{K} \ln R, \tag{5.1}$$

where R is the ratio of two ion saturation currents ($I(\pi)/I(0)$) and K is a constant of the order of unity. The difference between eqs.(2.6) and (5.1) is small and less than 10% for $1 \leq R \leq 3$ with $K = 2\alpha = 1$ (see Fig. 8). In particular, when R is close to unity, $\ln R$ is approximated to $2(I(\pi) - I(0))/(I(\pi) + I(0))$, and eq.(5.1) is identical with eq.(2.6).

In the calibration method presented in §4.2, we have assumed that the perpendicular flow is entirely due to $E \times B$ drift, and neglected the diamagnetic and centrifugal effects. Here, we estimate the flow velocity including these effects. From the radial component of the equation of motion in cylindrical coordinates, the azimuthal drift velocity is given by

$$v_\theta = \frac{r\omega_{ci}}{2}\left[-1 + \sqrt{1 + \frac{4}{r\omega_{ci}^2}\left(C_s^2 \frac{\partial \phi'}{\partial r} + v_{th}^2 \frac{\partial}{\partial r} \ln n\right)}\right], \tag{5.2}$$

where $\omega_{ci}(= eB/m_i)$ is the ion cyclotron frequency, $\phi'(= e\phi/T_e)$ the electric potential normalized to the electron temperature, and $v_{th}(= T_i/m_i)$ the ion thermal velocity, respectively. Since the angular frequencies of $E \times B$ drift and of diamagnetic drift are much smaller than ω_{ci}, we can expand the square root of eq.(5.2) to have

$$v_\theta = \frac{C_s^2}{\omega_{ci}} \frac{\partial \phi'}{\partial r} + \frac{v_{th}^2}{\omega_{ci}} \frac{\partial}{\partial r} \ln n - \frac{1}{r\omega_{ci}^3}\left(C_s^2 \frac{\partial \phi'}{\partial r} + v_{th}^2 \frac{\partial}{\partial r} \ln n\right)^2. \tag{5.3}$$

The first and second terms are the $E \times B$ drift velocity ($V_{E\times B}$) and the diamagnetic drift velocity (V_D), respectively, and the third term is the centrifugal correction term (V_C). The quantities $\partial\phi'/\partial r$ and $\partial \ln n/\partial r$ are of the same order, and thus $V_D/V_{E\times B} \sim T_i/T_e \ll 1$. The centrifugal correction, $V_C \sim (\omega_{E\times B}/\omega_{ci})V_{E\times B}$, is also negligible compared with the $E \times B$ drift velocity, where $\omega_{E\times B}$ is the angular frequency of $E \times B$ rotation ($V_{E\times B}/r$). For the present experimental conditions, the perpendicular motion of ions is entirely due to the $E \times B$ drift.

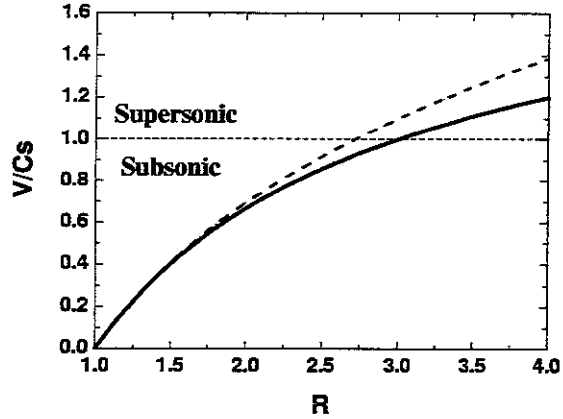

Fig. 8. Comparison between $\Delta I/ < I >$ (solid line) and $\ln R$ (dashed line), where R is $I(\pi)/I(0)$. The coefficients are taken to be $2\alpha = K = 1$.

§6. Conclusion

It is both experimentally and theoretically shown that the effect of magnetic field on a directional Langmuir probe can be completely eliminated, and the flow velocity directed to an arbitrary angle with respect to magnetic field can be measured. An *in situ* calibration method is proposed to determine the absolute flow velocity, and successfully demonstrated to measure the perpendicular flow velocity. The applicability limit of the present method to strongly ion-magnetized cases is experimentally examined, and found to be $\rho_i/r_p \sim 1$, which is understood as the onset of flow disturbance induced by the probe. In the present work, we *a priori* assumed subsonic cases ($V/C_s < 1$) although there is no explicit limit on the magnitude of flow velocity in the theory. It is very interesting and also important to know whether or not the proportionality relation between flow velocity and quantity $(I(\theta+\pi) - I(\theta))/(I(\theta+\pi) + I(\theta))$ still holds in supersonic regimes, which is left for future study.

Acknowledgements

One of the authors (K. N.) would like to thank Profs. R. Hatakeyama and M. Inutake for helpful discussions. He also wishes to thank Prof. A. Tsushima for useful suggestions and continuous encouragement.

1) P. C. Stangeby, Phys. Fluids. **27**, 2699 (1984).
2) I. H. Hutchinson, Phys. Fluids. **30**, 3777 (1987)
3) K-S. Chung and I. H. Hutchinson, Phys. Rev. A **38**, 4721 (1988).
4) H. Amemiya, A. Tsushima and G. Fuchs, Contrib. Plasma Phys. **39**, 515 (1999).
5) H. Van Goubergen, R. R. Weynants, S. Jachmich, M. Van Schoor, G. Van Oost and E. Desoppere, Plasma Phys. Control. Fusion, **41**, L17 (1999).
6) R. Hatakeyama, N. Hershkowitz, R. Majeski, Y. J. Wen, D B. Brouchous, P. Proberts, R. A. Breun, D. Roberts, M. Vukovic and T. Tanaka, Phys. Plasmas. **4**, 2947 (1997).
7) M. Hudis and L. M. Lidsky, J. Appl. Phys. **41**, 5011 (1970).
8) I. H. Hutchinson, Phys. Rev. A **A37**, 4358 (1988).
9) K-S. Chung, I. H. Hutchinson, B. LaBombard and R. W. Conn, Phys. Fluids. **B1**, 2229 (1989).
10) K-S. Chung and I. H. Hutchinson, Phys. Fluids. **B3**, 3053 (1991).
11) R. J. Armstrong and D. S. Darrow, Nucl. Fusion **34**, 1532 (1994).
12) V. Antoni, D. Desideri, E. Martines, G. Serianni and L. Tramontin, Nucl. Fusion. **36**, 1561 (1996).
13) Y. Amagishi and T. Miyazaki, J. Phys. Soc. Jpn **67**, 3774(1998).

Recent Issues of NIFS Series

NIFS-571 A. Iiyoshi, A. Komori, A. Ejiri, M. Emoto, H. Funaba, M. Goto, K. Ida, H. Idei, S. Inagaki, S. Kado, O. Kaneko, K. Kawahata, S. Kubo, R. Kumazawa, S. Masuzaki, T. Minami, J. Miyazawa, T. Morisaki, S. Morita, S. Murakami, S. Muto, T. Muto, Y. Nagayama, Y. Nakamura, H. Nakanishi, K. Narihara, K. Nishimura, N. Noda, T. Kobuchi, S. Ohdachi, N. Ohyabu, Y. Oka, M. Osakabe, T. Ozaki, B.J. Peterson, A. Sagara, S. Sakakibara, R. Sakamoto, H. Sasao, M. Sasao, K. Sato, M. Sato, T. Seki, T. Shimozuma, M. Shoji, H. Suzuki, Y. Takeiri, K. Tanaka, K. Toi, T. Tokuzawa, K. Tsumori, I. Yamada, H. Yamada, S. Yamaguchi, M. Yokoyama, K.Y. Watanabe, T. Watari, R. Akiyama, H. Chikaraishi, K. Haba, S. Hamaguchi, S. Iima, S. Imagawa, N. Inoue, K. Iwamoto, S. Kitagawa, Y. Kubota, J. Kodaira, R. Maekawa, T. Mito, T. Nagasaka, A. Nishimura, Y. Takita, C. Takahashi, K. Takahata, K. Yamauchi, H. Tamura, T. Tsuzuki, S. Yamada, N. Yanagi, H. Yonezu, Y. Hamada, K. Matsuoka, K. Murai, K. Ohkubo, I. Ohtake, M. Okamoto, S. Sato, T. Satow, S. Sudo, S. Tanahashi, K. Yamazaki, M. Fujiwara and O. Motojima,
An Overview of the Large Helical Device Project; Oct. 1998
(IAEA-CN-69/OV1/4)

NIFS-572 M. Fujiwara, H. Yamada, A. Ejiri, M. Emoto, H. Funaba, M. Goto, K. Ida, H. Idei, S. Inagaki, S. Kado, O. Kaneko, K. Kawahata, A. Komori, S. Kubo, R. Kumazawa, S. Masuzaki, T. Minami, J. Miyazawa, T. Morisaki, S. Morita, S. Murakami, S. Muto, T. Muto, Y. Nagayama, Y. Nakamura, H. Nakanishi, K. Narihara, K. Nishimura, N. Noda, T. Kobuchi, S. Ohdachi, N. Ohyabu, Y. Oka, M. Osakabe, T. Ozaki, B. J. Peterson, A. Sagara, S. Sakakibara, R. Sakamoto, H. Sasao, M. Sasao, K. Sato, M. Sato, T. Seki, T. Shimozuma, M. Shoji, H. Sazuki, Y. Takeiri, K. Tanaka, K. Toi, T. Tokuzawa, K. Tsumori, I. Yamada, S. Yamaguchi, M. Yokoyama, K.Y. Watanabe, T. Watari, R. Akiyama, H. Chikaraishi, K. Haba, S. Hamaguchi, M. Iima, S. Imagawa, N. Inoue, K. Iwamoto, S. Kitagawa, Y. Kubota, J. Kodaira, R. Maekawa, T. Mito, T. Nagasaka, A. Nishimura, Y. Takita, C. Takahashi, K. Takahata, K. Yamauchi, H. Tamura, T. Tsuzuki, S. Yamada, N. Yanagi, H. Yonezu, Y. Hamada, K. Matsuoka, K. Murai, K. Ohkubo, I. Ohtake, M. Okamoto, S. Sato, T. Satow, S. Sudo, S. Tanahashi, K. Yamazaki, O. Motojima and A. Iiyoshi,
Plasma Confinement Studies in LHD; Oct. 1998
(IAEA-CN-69/EX2/3)

NIFS-573 O. Motojima, K. Akaishi, H. Chikaraishi, H. Funaba, S. Hamaguchi, S. Imagawa, S. Inagaki, N. Inoue, A. Iwamoto, S. Kitagawa, A. Komori, Y. Kubota, R. Maekawa, S. Masuzaki, T. Mito, J. Miyazawa, T. Morisaki, T. Muroga, T. Nagasaka, Y. Nakmura, A. Nishimura, K. Nishimura, N. Noda, N. Ohyabu, S. Sagara, S. Sakakibara, R. Sakamoto, S. Satoh, T. Satow, M. Shoji, H. Suzuki, K. Takahata, H. Tamura, K. Watanabe, H. Yamada, S. Yamada, S. Yamaguchi, K. Yamazaki, N. Yanagi, T. Baba, H. Hayashi, M. Iima, T. Inoue, S. Kato, T. Kato, T. Kondo, S. Moriuchi, H. Ogawa, I. Ohtake, K. Ooba, H. Sekiguchi, N. Suzuki, S. Takami, Y. Taniguchi, T. Tsuzuki, N. Yamamoto, K. Yasui, H. Yonezu, M. Fujiwara and A. Iiyoshi,
Progress Summary of LHD Engineering Design and Construction; Oct. 1998
(IAEA-CN-69/FT2/1)

NIFS-574 K. Toi, M. Takechi, S. Takagi, G. Matsunaga, M. Isobe, T. Kondo, M. Sasao, D.S. Darrow, K. Ohkuni, S. Ohdachi, R. Akiyama, A. Fujisawa, M. Gotoh, H. Idei, K. Ida, H. Iguchi, S. Kado, M. Kojima, S. Kubo, S. Lee, K. Matsuoka, T. Minami, S. Morita, N. Nikai, S. Nishimura, S. Okamura, M. Osakabe, A. Shimizu, Y. Shirai, C. Takahashi, K. Tanaka, T. Watari and Y. Yoshimura,
Global MHD Modes Excited by Energetic Ions in Heliotron/Torsatron Plasmas; Oct. 1998
(IAEA-CN-69/EXP1/19)

NIFS-575 Y. Hamada, A. Nishizawa, Y. Kawasumi, A. Fujisawa, M. Kojima, K. Narihara, K. Ida, A. Ejiri, S. Ohdachi, K. Kawahata, K. Toi, K. Sato, T. Seki, H. Iguchi, K. Adachi, S. Hidekuma, S. Hirokura, K. Iwasaki, T. Ido, R. Kumazawa, H. Kuramoto, T. Minami, I. Nomura, M. Sasao, K.N. Sato, T. Tsuzuki, I. Yamada and T. Watari,
Potential Turbulence in Tokamak Plasmas; Oct. 1998
(IAEA-CN-69/EXP2/14)

NIFS-576 S. Murakami, U. Gasparino, H. Idei, S. Kubo, H. Maassberg, N. Marushchenko, N. Nakajima, M. Romé and M. Okamoto,
5D Simulation Study of Suprathermal Electron Transport in Non-Axisymmetric Plasmas, Oct. 1998
(IAEA-CN-69/THP1/01)

NIFS-577 S. Fujiwara and T. Sato,
Molecular Dynamics Simulation of Structure Formation of Short Chain Molecules; Nov. 1998

NIFS-578 T. Yamagishi,
Eigenfunctions for Vlasov Equation in Multi-species Plasmas Nov. 1998

NIFS-579 M. Tanaka, A. Yu. Grosberg and T. Tanaka,
Molecular Dynamics of Strongly-Coupled Multichain Coulomb Polymers in Pure and Salt Aqueous Solutions; Nov. 1998

NIFS-580 J. Chen, N. Nakajima and M. Okamoto,
Global Mode Analysis of Ideal MHD Modes in a Heliotron/Torsatron System: I. Mercier-unstable Equilibria; Dec. 1998

NIFS-581 M. Tanaka, A. Yu. Grosberg and T. Tanaka,
Comparison of Multichain Coulomb Polymers in Isolated and Periodic Systems: Molecular Dynamics Study; Jan. 1999

NIFS-582 V.S. Chan and S. Murakami,

Self-Consistent Electric Field Effect on Electron Transport of ECH Plasmas; Feb. 1999

NIFS-583 M. Yokoyama, N. Nakajima, M. Okamoto, Y. Nakamura and M. Wakatani,
Roles of Bumpy Field on Collisionless Particle Confinement in Helical-Axis Heliotrons; Feb. 1999

NIFS-584 T-H. Watanabe, T. Hayashi, T. Sato, M. Yamada and H. Ji,
Modeling of Magnetic Island Formation in Magnetic Reconnection Experiment; Feb. 1999

NIFS-585 R. Kumazawa, T. Mutoh, T. Seki, F. Shinpo, G. Nomura, T. Ido, T. Watari, Jean-Marie Noterdaeme and Yangping Zhao,
Liquid Stub Tuner for Ion Cyclotron Heating; Mar. 1999

NIFS-586 A. Sagara, M. Iima, S. Inagaki, N. Inoue, H. Suzuki, K. Tsuzuki, S. Masuzaki, J. Miyazawa, S. Morita, Y. Nakamura, N. Noda, B. Peterson, S. Sakakibara, T. Shimozuma, H. Yamada, K. Akaishi, H. Chikaraishi, H. Funaba, O. Kaneko, K. Kawahata, A. Komori, N. Ohyabu, O. Motojima, LHD Exp. Group 1, LHD Exp. Group 2,
Wall Conditioning at the Starting Phase of LHD; Mar. 1999

NIFS-587 T. Nakamura and T. Yabe,
Cubic Interpolated Propagation Scheme for Solving the Hyper-Dimensional Vlasov-Poisson Equation in Phase Space; Mar. 1999

NIFS-588 W.X. Wnag, N. Nakajima, S. Murakami and M. Okamoto,
An Accurate δf Method for Neoclassical Transport Calculation; Mar. 1999

NIFS-589 K. Kishida, K. Araki, S. Kishiba and K. Suzuki,
Local or Nonlocal? Orthonormal Divergence-free Wavelet Analysis of Nonlinear Interactions in Turbulence, Mar 1999

NIFS-590 K. Araki, K. Suzuki, K. Kishida and S. Kishiba,
Multiresolution Approximation of the Vector Fields on T^3; Mar. 1999

NIFS-591 K. Yamazaki, H. Yamada, K.Y.Watanabe, K. Nishimura, S. Yamaguchi, H. Nakanishi, A. Komori, H. Suzuki, T. Mito, H. Chikaraishi, K. Murai, O. Motojima and the LHD Group,
Overview of the Large Helical Device (LHD) Control System and Its First Operation; Apr. 1999

NIFS-592 T. Takahashi and Y. Nakao,
Thermonuclear Reactivity of D-T Fusion Plasma with Spin-Polarized Fuel; Apr. 1999

NIFS-593 H. Sugama,
Damping of Toroidal Ion Temperature Gradient Modes; Apr. 1999

NIFS-594 Xiaodong Li,
Analysis of Crowbar Action of High Voltage DC Power Supply in the LHD ICRF System; Apr. 1999

NIFS-595 K. Nishimura, R. Horiuchi and T. Sato,
Drift-kink Instability Induced by Beam Ions in Field-reversed Configurations; Apr. 1999

NIFS-596 Y. Suzuki, T-H. Watanabe, T. Sato and T. Hayashi,
Three-dimensional Simulation Study of Compact Toroid Plasmoid Injection into Magnetized Plasmas; Apr. 1999

NIFS-597 H. Sanuki, K. Itoh, M. Yokoyama, A. Fujisawa, K. Ida, S. Toda, S.-I. Itoh, M. Yagi and A. Fukuyama,
Possibility of Internal Transport Barrier Formation and Electric Field Bifurcation in LHD Plasma; May 1999

NIFS-598 S. Nakazawa, N. Nakajima, M. Okamoto and N. Ohyabu,
One Dimensional Simulation on Stability of Detached Plasma in a Tokamak Divertor; June 1999

NIFS-599 S. Murakami, N. Nakajima, M. Okamoto and J. Nhrenberg,
Effect of Energetic Ion Loss on ICRF Heating Efficiency and Energy Confinement Time in Heliotrons; June 1999

NIFS-600 R. Horiuchi and T. Sato,
Three-Dimensional Particle Simulation of Plasma Instabilities and Collisionless Reconnection in a Current Sheet;; June 1999

NIFS-601 W. Wang, M. Okamoto, N. Nakajima and S. Murakami,
Collisional Transport in a Plasma with Steep Gradients, June 1999

NIFS-602 T. Mutoh, R. Kumazawa, T. Saki, K. Saito, F. Simpo, G. Nomura, T. Watari, X. Jikang, G. Cattanei, H. Okada, K. Ohkubo, M. Sato, S. Kubo, T. Shimozuma, H. Idei, Y. Yoshimura, O. Kaneko, Y. Takeiri, M. Osakabe, Y. Oka, K. Tsumori, A. Komori, H. Yamada, K. Watanabe, S. Sakakibara, M. Shoji, R. Sakamoto, S. Inagaki, J. Miyazawa, S. Morita, K. Tanaka, B.J. Peterson, S. Murakami, T. Minami, S. Ohdachi, S. Kado, K. Narihara, H. Sasao, H. Suzuki, K. Kawahata, N. Ohyabu, Y. Nakamura, H. Funaba, S. Masuzaki, S. Muto, K. Sato, T. Morisaki, S. Sudo, Y. Nagayama, T. Watanabe, M. Sasao, K. Ida, N. Noda, K. Yamazaki, K. Akaishi, A. Sagara, K. Nishimura, T. Ozaki, K. Toi, O. Motojima, M. Fujiwara, A. Iiyoshi and LHD Exp. Group 1 and 2,
First ICRF Heating Experiment in the Large Helical Device, July 1999

NIFS-603 P.C. de Vries, Y. Nagayama, K. Kawahata, S. Inagaki, H. Sasao and K. Nagasaki,
Polarization of Electron Cyclotron Emission Spectra in LHD, July 1999

NIFS-604 W. Wang, N. Nakajima, M. Okamoto and S. Murakami,
δf Simulation of Ion Neoclassical Transport; July 1999

NIFS-605 T. Hayashi, N. Mizuguchi, T. Sato and the Complexity Simulation Group,
Numerical Simulation of Internal Reconnection Event in Spherical Tokamak; July 1999

NIFS-606 M. Okamoto, N. Nakajima and W. Wang,
On the Two Weighting Scheme for δf Collisional Transport Simulation; Aug. 1999

NIFS-607 O. Motojima, A.A. Shishkin, S. Inagaki, K.Y. Watanabe,
Possible Control Scenario of Radial Electric Field by Loss-Cone-Particle Injection into Helical Device; Aug. 1999

NIFS-608 R. Tanaka, T. Nakamura and T. Yabe,
Constructing Exactly Conservative Scheme in Non-conservative Form; Aug. 1999

NIFS-609 H. Sugama,
Gyrokinetic Field Theory; Aug. 1999

NIFS-610 M. Takechi, G. Matsunaga, S. Takagi, K.Ohkuni, K. Toi, M. Osakabe, M. Isobe, S. Okamura, K. Matsuoka, A. Fujisawa, H. Iguchi, S. Lee, T. Minami, K. Tanaka, Y. Yoshimura and CHS Group,
Core Localized Toroidal Alfven Eigenmodes Destabilized By Energetic Ions in the CHS Heliotron/Torsatron; Sep. 1999

NIFS-611 K. Ichiguchi,
MHD Equilibrium and Stability in Heliotron Plasmas; Sep. 1999

NIFS-612 Y. Sato, M. Yokoyama, M. Wakatani and V. D. Pusovitov,
Complete Suppression of Pfirsch-Schluter Current in a Toroidal l=3 Stellarator; Oct. 1999

NIFS-613 S. Wang, H. Sanuki and H. Sugama,
Reduced Drift Kinetic Equation for Neoclassical Transport of Helical Plasmas in Ultra-low Collisionality Regime; Oct. 1999

NIFS-614 J. Miyazawa, H. Yamada, K. Yasui, S. Kato, N., Fukumoto, M. Nagata and T. Uyama,
Design of Spheromak Injector Using Conical Accelerator for Large Helical Device; Nov. 1999

NIFS-615 M. Uchida, A. Fukuyama, K. Itoh, S.-I. Itoh and M. Yagi,
Analysis of Current Diffusive Ballooning Mode in Tokamaks; Dec. 1999

NIFS-616 M. Tanaka, A.Yu. Grosberg and T. Tanaka,
Condensation and Swelling Behavior of Randomly Charged Multichain Polymers by Molecular Dynamics Simulations; Dec. 1999

NIFS-617 S. Goto and S. Kida,
Sparseness of Nonlinear Coupling, Dec. 1999

NIFS-618 M.M. Skoric, T. Sato, A. Maluckov and M.S. Jovanovic,
Complexity in Laser Plasma Instabilities Dec. 1999

NIFS-619 T.-H. Watanabe, H. Sugama and T. Sato,
Non-dissipative Kinetic Simulation and Analytical Solution of Three-mode Equations of Ion Temperature

Gradient Instability; Dec. 1999

NIFS-620 Y. Oka, Y. Takeiri, Yu.I.Belchenko, M. Hamabe, O. Kaneko, K. Tsumori, M. Osakabe, E. Asano, T. Kawamoto, R. Akiyama,
Optimization of Cs Deposition in the 1/3 Scale Hydrogen Negative Ion Source for LHD-NBI System ;Dec. 1999

NIFS-621 Yu.I. Belchenko, Y. Oka, O. Kaneko, Y. Takeiri, A. Krivenko, M. Osakabe, K. Tsumori, E. Asano, T Kawamoto, R. Akiyama,
Recovery of Cesium in the Hydrogen Negative Ion Sources;Dec. 1999

NIFS-622 Y. Oka, O. Kaneko, K. Tsumori, Y. Takeiri, M. Osakabe, T. Kawamoto, E Asano, and R. Akiyama,
H- Ion Source Using a Localized Virtual Magnetic Filter in the Plasma Electrode: Type I LV Magnetic Filter: Dec. 1999

NIFS-623 M. Tanaka, S Kida, S. Yanase and G. Kawahara,
Zero-absolute-vorticity State in a Rotating Turbulent Shear Flow, Jan 2000

NIFS-624 F. Leuterer, S. Kubo,
Electron Cyclotron Current Drive at $\omega \approx \omega_c$ with X-mode Launched from the Low Field Side; Feb. 2000

NIFS-625 K Nishimura,
Wakefield of a Charged Particulate Influenced by Emission Process of Secondary Electrons; Mar. 2000

NIFS-626 K Itoh, M. Yagi, S.-I. Itoh, A Fukuyama,
On Turbulent Transport in Burning Plasmas;Mar. 2000

NIFS-627 K Itoh, S.-I. Itoh, L. Giannone,
Modelling of Density Limit Phenomena in Toroidal Helical Plasmas; Mar 2000

NIFS-628 K Akaishi, M. Nakasuga and Y. Funato,
True and Measured Outgassing Rates of a Vacuum Chamber with a Reversibly Absorbed Phase;Mar. 2000

NIFS-629 T. Yamagishi,
Effect of Weak Dissipation on a Drift Orbit Mapping; Mar. 2000

NIFS-630 S. Toda, S.-I, Itoh, M. Yagi, A Fukuyama and K Itoh,
Spatial Structure of Compound Dither in L/H Transition;Mar. 2000

NIFS-631 N. Ishihara and S. Kida,
Axial and Equatorial Magnetic Dipoles Generated in a Rotating Spherical Shell; Mar. 2000

NIFS-632 T. Kuroda, H. Sugama, R. Kanno and M. Okamoto,
Ion Temperature Gradient Modes in Toroidal Helical Systems; Apr. 2000

NIFS-633 V.D. Pustovitov,
Magnetic Diagnostics: General Principles and the Problem of Reconstruction of Plasma Current and Pressure Profiles in Toroidal Systems, Apr. 2000

NIFS-634 A.B. Mikhailovskii, S.V. Konovalov, V.D. Pustovitov and V.S. Tsypin,
Mechanism of Viscosity Effect on Magnetic Island Rotation, Apr. 2000

NIFS-635 H. Naitou, T. Kuramoto, T. Kobayashi, M. Yagi, S. Tokuda and T. Matsumoto,
Stabilization of Kinetic Internal Kink Mode by Ion Diamagnetic Effects; Apr. 2000

NIFS-636 A. Kageyama and S. Kida,
A Spectral Method in Spherical Coordinates with Coordinate Singularity at the Origin; Apr 2000

NIFS-637 R. Horiuchi, W. Pei and T. Sato,
Collisionless Driven Reconnection in an Open System;June. 2000

NIFS-638 K Nagaoka, A Okamoto, S. Yoshimura and M.Y Tanaka,
Plasma Flow Measurement Using Directional Langmuir Probe under Weakly Ion-Magnetized Conditions; July 2000